IOPscience iopscience.iop.org

Home Search Collections Journals About Contact us My IOPscience

Spin warp NMR imaging and applications to human whole-body imaging

This content has been downloaded from IOPscience. Please scroll down to see the full text.

1980 Phys. Med. Biol. 25 751

(http://iopscience.iop.org/0031-9155/25/4/017)

View the table of contents for this issue, or go to the journal homepage for more

Download details:

IP Address: 152.11.5.70
This content was downloaded on 12/03/2014 at 22:32

Please note that terms and conditions apply.

While no definite explanations can be offered for these variations in ratio of T_1 values for different tissues, it is suggested that they may be associated with differences in the histological structure of the tissues. In particular it is noticeable that nervous tissues which contain a large quantity of myelin have low ratios, and the actual decrease in ratio from the general value seems, to some extent, to reflect the increase in the amount of the myelin membranes in the tissue sample.

Work is continuing to investigate both the relationship between these changes in the T_1 relaxation time ratios at different frequencies and the fundamental mechanisms of T_1 relaxation in tissue, and also to see what effect, if any, this phenomenon is likely to have in the production or interpretation of T_1 relaxation images of living systems.

We would like to thank Professor J. R. Mallard for his encouragement, and to acknowledge financial support from The Grampian Health Board.

C Rosemary Ling, Margaret A Foster
and J M S Hutchison,
Department of Bio-Medical Physics and
Bio-Engineering,
University of Aberdeen, Foresterhill,
Aberdeen AB9 2ZD, Scotland

31 *March* 1980

References

Coles B A 1976 *J. Natl. Cancer Inst.* **57** 389–93
Gadian D G 1977 *Contemp. Phys.* **18** 351–72

Spin warp NMR imaging and applications to human whole-body imaging†

The Editor,
Sir,

In this letter we describe a new nuclear magnetic resonance (NMR) imaging technique which we call 'spin warp imaging' and we give examples of its application to human whole-body imaging.

Our apparatus is based on a four-coil, air cored magnet (made by the Oxford Instrument Company) capable of accepting the whole human body. The magnet produces a static field of 0·04 T giving a proton NMR frequency of 1·7 MHz. The maximum field inhomogeneity is about 6×10^{-4} at a radius of 0·23 m, approximately twice the amount theoretically attainable with this configuration. The apparatus will be described in detail in a forthcoming publication (Hutchison *et al* 1980).

The pulse sequence we use for our new imaging method is shown in figure 1. This refers to a set of coordinate axes with z vertical along the static field, y horizontal along the long axis of the patient, and x horizontal across the patient.

† This device is the subject of Patent Applications 25899/78, 40779/78, 79/34864, 80/08773, by the National Research Development Corporation.

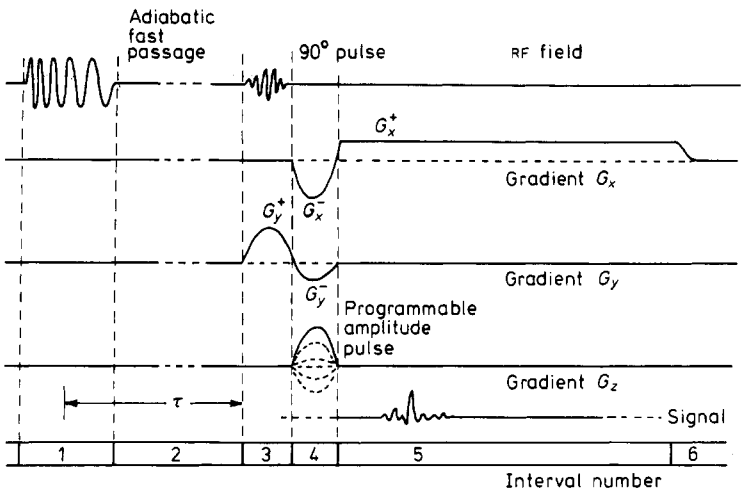

Figure 1. Spin warp imaging pulse sequence.

If we concentrate on the events beginning at interval 3, the major functions of this sequence are a selective 90° excitation of a thin slab of spins perpendicular to the y axis, projection of the spin density onto the x axis, and phase encoding of the spins in the z direction to allow spatial discrimination along z.

The plane selection is done by a combination of the Gaussian shaped, narrow-band radiofrequency (RF) pulse in interval 3 along with the application of a magnetic field gradient G_y^+ (peak value $2{\cdot}7\ \mathrm{mT\,m^{-1}}$). The plane selection is completed by the negative, rephasing G_y^- lobe in interval 4.

The projection of the spin density onto the x axis is accomplished by an initial dephasing G_x^- in interval 4 followed by a positive, constant G_x^+ gradient ($0{\cdot}5\ \mathrm{mT\,m^{-1}}$) in interval 5, which produces a spin echo signal. If the signal is sampled M times, with due consideration for bandwidth requirements, then the Fourier transform of the signal will be a complex M-point projection of the sample spin density onto the x axis.

Phase encoding in the z direction is achieved by the application of a half-sine-wave pulse G_z in interval 4. G_z is applied for the same time in each pulse sequence, but its strength is varied to satisfy the integral condition

$$\gamma L_z \int_4 \mathrm{d}t\, G_z = 2\pi n \tag{1}$$

where γ is the gyromagnetic ratio, L_z is the total length of the sample in the z direction, $\int_4 \mathrm{d}t$ is the integral over interval 4, and n is an integer. In order to distinguish N regions in the vertical direction, it is necessary to take N signals with, for example, $n = -\frac{1}{2}N$, $-\frac{1}{2}N+1, \ldots, -1, 0, 1, \ldots \frac{1}{2}N-1$. A two-dimensional Fourier transform of the N signals will then produce an $M \times N$ image of the spin density in the selected plane.

Another view of the action of the phase-encoding gradient is that in each imaging column we are collecting n projections onto the x axis. The projections are different because spins at different heights are given varying amounts of phase twist by the different G_z's (hence the name 'spin warp'). This situation differs from X-ray CAT scanning where only density (and not phase) information is available, in which case the n projections must be taken from n different angles.

Signals derived from the events of interval 3 onwards are called S1 signals and contain mostly proton density information.

Spin-lattice relaxation time (T_1) information can be obtained by starting the sequence at interval 1. The spins are inverted and one waits during interval 2 for a time τ approximately equal to the average relaxation time in the sample (200 ms). The above described sequence starting with interval 3 is then performed. This is similar to the standard 180°-τ-90° sequence for measuring T_1. The initial inversion is done here by using an adiabatic fast passage, for which the RF magnetic field in the rotating frame is about 20 μT and sweeps from +8 kHz to −8 kHz relative to the central Larmor frequency in 10 ms, giving more than 90% inversion.

Signals derived from the pulse sequence starting with interval 1 are called S2 signals and contain both proton density and T_1 relaxation time information.

The above sequence is similar to one proposed by Richard Ernst and colleagues (Kumar *et al* 1975, Ernst 1978). However, in their proposal, changes in $\int dt\, G_z$ are achieved by applying a gradient of fixed strength for different time intervals, whereas we apply gradients of differing strengths for a fixed time interval. Ernst's method would appear to be impractical for whole-body imaging using a four coil magnet system like ours, since inhomogeneities in the static field simulate the effects of the applied G_z.

A numerical example, based on our system, will illustrate the problem. Setting $L_z = 0{\cdot}4$ m, $t = 0{\cdot}5$ ms, $\gamma/2\pi = 42{\cdot}6$ MHz T^{-1}, $\gamma L_z G_z t = 2\pi$ gives us $G_z \approx 100\ \mu\text{T m}^{-1}$. ($t$ is the shortest time interval for which the gradient G_z is switched on.) At 0·2 m, the maximum distance from the centre of the field, $G_z \times z = 20\ \mu$T. But the fractional inhomogeneity in our magnet at this radius is about 3×10^{-4}, or 12 μT, more than half the contribution of the applied gradient. This is unacceptable since we wish to resolve the 24 cm into 32 or more parts, and the distortion (and aliasing) introduced by such an inhomogeneity would ruin the image making process. Similar magnets with the same physical dimensions but higher fields will have the same fractional inhomogeneity and hence higher absolute inhomogeneity, thereby increasing the problem.

Looked at in a slightly different way, the above difficulty imposes a condition on the homogeneity of the static magnetic field.

In the present technique there is still an extra phase shift caused by the inhomogeneity, but that extra phase shift is the same for all pulse trains. This extra, constant phase shift for all signals cannot affect the linearity and scale in the z direction. This conclusion relaxes the stringent condition imposed on the static field homogeneity by Ernst's method.

Inhomogeneity will cause a horizontal nonlinearity. However, since G_x is not constrained by condition (1), it can be made large enough to overcome this effect; $0{\cdot}5\ \text{mT m}^{-1}$ gives reasonable geometry in the present case.

It is also instructive to compare the spin warp technique with NMR imaging by multiple-angle projections. In the latter case, inhomogeneities cause projected lines to be curved, thereby making reconstruction difficult. One must either know exactly the curvature of the projected lines from all the projected angles or else make the field very homogeneous. In the spin warp technique, all the projections are along the same direction, and therefore inhomogeneity will manifest itself only as a geometric distortion in the final image; there will be no smearing of imaging information. Calculations based on the actual parameters of a 4-coil magnet show the inherent inhomogeneities to be a serious problem for imaging by multiple-angle projections over a region large enough to accommodate the human trunk (Hutchison *et al* 1978).

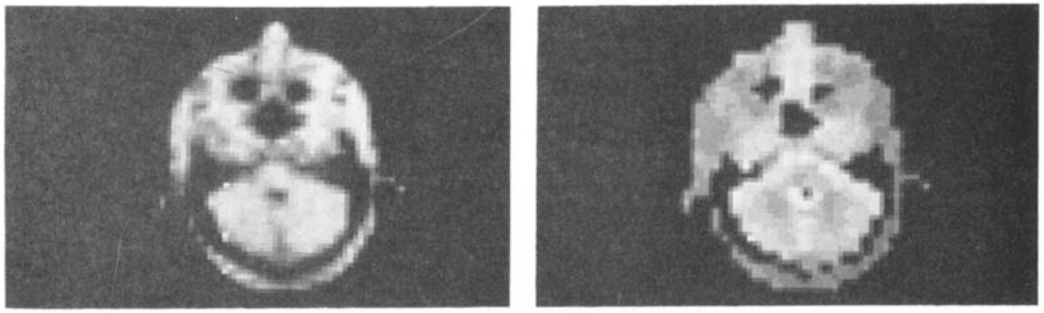

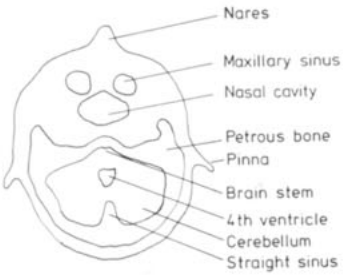
Nares
Maxillary sinus
Nasal cavity
Petrous bone
Pinna
Brain stem
4th ventricle
Cerebellum
Straight sinus

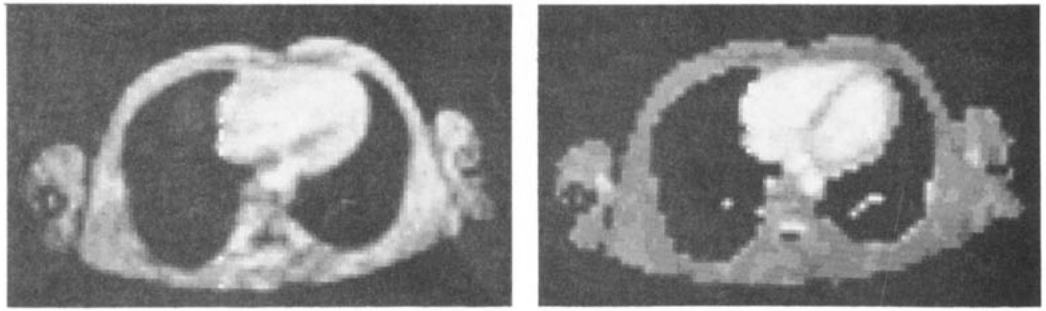

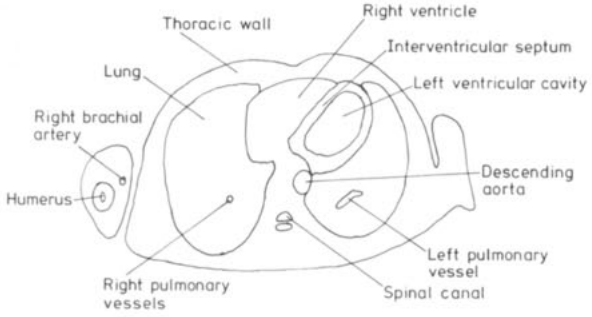
Thoracic wall
Right ventricle
Interventricular septum
Lung
Left ventricular cavity
Right brachial artery
Descending aorta
Humerus
Left pulmonary vessel
Right pulmonary vessels
Spinal canal

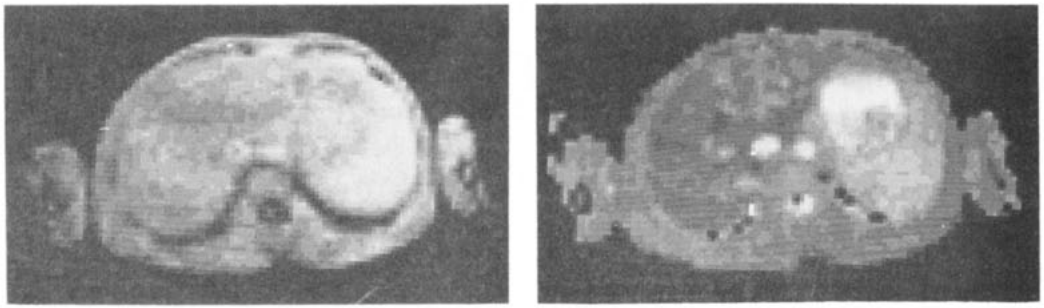

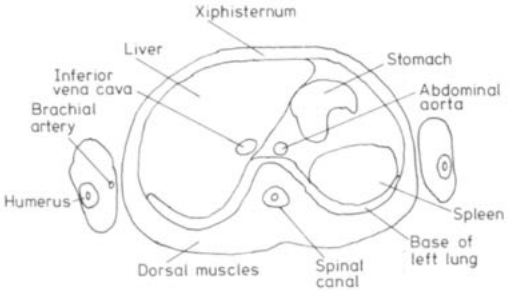
Xiphisternum
Liver
Stomach
Inferior vena cava
Abdominal aorta
Brachial artery
Humerus
Spleen
Base of left lung
Dorsal muscles
Spinal canal

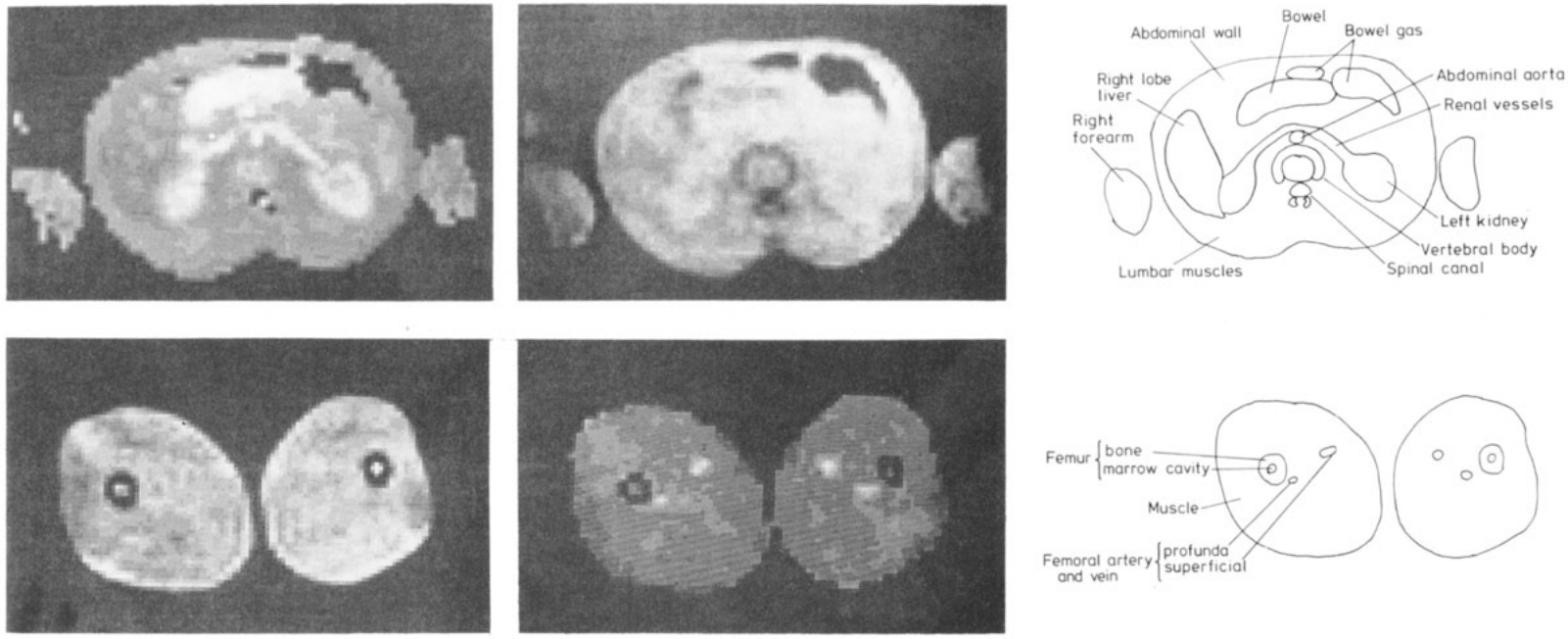

Figure 2. Tomographic sections through WAE. The three columns are respectively proton density images relaxation time (T_1) images and outlines of the important features. (*a*) Head section 25 mm below eyes. (*b*) Chest section through heart at level T8. (*c*) Abdominal section at level T10. (*d*) Abdominal section at level L2. (*e*) Thigh section.

Some images made using the spin warp technique are shown in figure 2. A 128 s scan collects data for both a proton density and T_1 image. Such a scan consists of 64 signals of type S1 and 64 signals of type S2. One echo signal is collected each second. Initially, the S1 data and the (S1–S2) data are Fourier transformed into two 64×64 element arrays, in which each imaging element is 7·5 mm wide by 7·5 mm high by 18·5 mm deep (the slab thickness), composing a volume of 1 cm^3. The T_1 value for each imaging element is calculated from the formula $T_1 = 200/\ln[2 \times S1/(S1-S2)]$. The 64×64 element S1 and T_1 arrays are then interpolated into 128×128 arrays and displayed on a television monitor using 16 colour or grey levels.

The signal to noise ratio was measured by taking a scan through a thigh section and then repeating the scan with the radiofrequency transmitter off. For thigh muscle tissue this yielded a proton density uncertainty of 2·5% for a 1 cm^3 tissue volume. The uncertainty in T_1 for any soft tissue with the same density as muscle tissue would be about 3·4% for T_1 around 200 ms with some worsening as the T_1 departs from that optimum value. These figures do not take into account possible aliasing, that is, the appearance of signal from part of the sample in the wrong part of the image.

As a general comment, we would point out that the T_1 images display more interesting detail than do the proton density ones. This is because the possible contrast among soft tissues is much greater if T_1 is used as the imaging parameter (Hutchison *et al* 1980), even though the uncertainty in T_1 is slightly greater than the uncertainty in proton density. It also seems likely that T_1 will be a parameter sensitive to changes produced by many diseases (Damadian 1971, Mallard *et al* 1980).

We acknowledge the financial support of the University of Aberdeen and the Medical Research Council under grant G975/937. We thank Professor J R Mallard for his interest and assistance and Dr F W Smith for his help in interpreting our images.

W A Edelstein, J M S Hutchison,
G Johnson and T Redpath,
Dept of Bio-Medical Physics
and Bio-Engineering,
University of Aberdeen,
Aberdeen,
Scotland, UK

12 *May* 1980

References

Damadian R 1971 *Science, NY* **171** 1151–3
Ernst R R 1978 *US Patent No.* 4070611
Hutchison J M S, Edelstein W A and Johnson G 1980 *J. Phys. E: Sci. Instrum.* in press
Hutchison J M S, Sutherland R J and Mallard J R 1978 *J. Phys. E: Sci. Instrum.* **11** 217–21
Kumar A, Welti D and Ernst R R 1975 *J. Magn. Reson.* **18** 69–83
Mallard J R, Hutchison J M S, Edelstein W A, Ling C R, Foster M A and Johnson G 1980 *Phil. Trans.* in press